Metabolism of albendazole, ricobendazole and flubendazole in *Haemonchus contortus* adults: Sex differences, resistance-related differences and the identification of new metabolites

Lucie Raisová Stuchlíková[a], Petra Matoušková[a], Ivan Vokřál[b], Jiří Lamka[b], Barbora Szotáková[a], Anna Sečkařová[a], Diana Dimunová[a], Linh Thuy Nguyen[a], Marián Várady[c], Lenka Skálová[a,*]

[a] *Department of Biochemical Sciences, Faculty of Pharmacy, Charles University, Heyrovského 1203, Hradec Králové, Czech Republic*
[b] *Department of Pharmacology and Toxicology, Faculty of Pharmacy, Charles University, Heyrovského 1203, Hradec Králové, Czech Republic*
[c] *Institute of Parasitology, Slovak Academy of Sciences, Hlinkova 3, Košice, Slovakia*

A R T I C L E I N F O

A B S T R A C T

Haemonchus contortus (family *Trichostrongylidae, Nematoda)*, a hematophagous gastrointestinal parasite found in small ruminants, has a great ability to develop resistance to anthelmintic drugs. We studied the biotransformation of the three benzimidazole anthelmintics: albendazole (ABZ), ricobendazole (albendazole S-oxide; RCB) and flubendazole (FLU) in females and males of *H. contortus* in both a susceptible ISE strain and resistant IRE strain. The *ex vivo* cultivation of living nematodes in culture medium with or without the anthelmintics was used. Ultrasensitive UHPLC/MS/MS analysis revealed 9, 7 and 12 metabolites of ABZ, RCB and FLU, respectively, with most of these metabolites now described in the present study for the first time in *H. contortus*. The structure of certain metabolites shows the presence of biotransformation reactions not previously reported in nematodes. There were significant qualitative and semi-quantitative differences in the metabolites formed by male and female worms. In most cases, females metabolized drugs more extensively than males. Adults of the IRE strain were able to form many more metabolites of all the drugs than adults of the ISE strain. Some metabolites were even found only in adults of the IRE strain. These findings suggest that increased drug metabolism may play a role in resistance to benzimidazole drugs in *H. contortus*.

1. Introduction

Haemonchus contortus (family *Trichostrongylidae, Nematoda)* is a hematophagous gastrointestinal parasite found in small ruminants that causes substantial economic losses to livestock production worldwide (Kaminsky et al., 2008). *H. contortus* has a great ability to develop resistance to anthelmintics (Kotze and Prichard, 2016), with drug resistance having become a major obstacle which threatens farm production and the welfare of the animals. Among parasites, the recent emergence of drug resistance to currently available drugs has raised serious problems for the control strategies and eventual elimination of parasitic diseases (Choe et al., 2012; Taman and Azab, 2014; Srivastava and Misra-Bhattacharya, 2015). The development of variable degrees of resistance among nematodes has been reported for all groups of anthelmintic drugs and increased level of resistance should be expected due to the considerable rise in drug administration, which increased drug pressure toward the selection of resistance alleles (Geary, 2012). The fact that resistance to monepantel, the latest anthelmintic in use,

has occurred within less than four years of the product first being introduced, is certainly a disquieting warning sign (Raza et al., 2016a; Sales and Love, 2016).

Mechanisms of drug resistance can be divided into pharmacodynamic-mediated and pharmacokinetic-mediated. The first type includes processes such as a decrease in the amount of target macromolecules or changes in their structures, both of which cause a reduction in drug efficacy. In the case of benzimidazole anthelmintics, the occurrence of single nucleotide polymorphisms within three codons (167, 198, and 200) of the β-tubulin isotype-1 gene, which change the three-dimensional structure of the beta tubulin protein target of benzimidazoles, has been demonstrated as the primary mechanism of resistance (Lubega and Prichard, 1990; Lubega and Prichard, 1991; Chaudhry et al., 2015).

Pharmacokinetic-mediated mechanisms may involve decreased drug uptake, accelerated drug efflux and increased drug inactivation. In this way, the concentration of the active drug within parasite cells is decreased, a lower number of drug molecules are able to bind to target macromolecules, thus the drug effect is reduced (Fernando et al., 2016;

Matouskova et al., 2016; Raza et al., 2016b). Pharmacokinetic-mediated drug resistance is based on an increase in the expression and activities of xenobiotic-metabolizing enzymes. In all organisms, these proteins serve as an efficient defense against the potential negative action of drugs and other xenobiotics. Several studies have described evidence of a direct association between xenobiotic-metabolizing enzymes and drug resistance in nematodes (reviewed in (Brophy et al., 2012; Matouskova et al., 2016)).

Our previous studies showed that *H. contortus* adults were able to metabolize the anthelmintic drugs albendazole (ABZ) and flubendazole (FLU) (Vokral et al., 2012; Vokral et al., 2013). ABZ-sulphoxide, ABZ-*N*-glucosides, FLU with reduced carbonyl group (FLU-R), FLU-*N*-glucosides and FLU-R-*O*-glucosides were identified in *H. contortus* adults incubated with ABZ and FLU, respectively. When the metabolisms of ABZ and FLU were compared in *H. contortus* strains sensitive and resistant to anthelmintics, a more pronounced glucosidation of both anthelmintics was found in the resistant strain. This finding indicates that drug deactivation via glucosidation could be one mechanism of resistance to benzimidazole anthelmintics in nematodes.

Nevertheless, a mix of adults of both sexes was used in these studies despite possible sex-differences in drug metabolism. Moreover, the analytical instruments available at the time of these experiments were less sensitive than present ones. Based on these particulars, the present study was designed to compare the metabolism of anthelmintics in females and males of *H. contortus* adults of an ISE (Inbred-Susceptible-Edinburg, MHco3) strain, which is susceptible to all main classes of anthelmintics (Roos et al., 2004), and a resistant IRE (Inbred-Resistant-Edinburgh; MHco5) strain (Yilmaz et al., 2017), which was directly developed from the ISE strain by imposing benzimidazole drug selection pressure. The metabolism of three benzimidazole anthelmintics was studied. In addition to ABZ and FLU, also ABZ-S-oxide (ABZSO; an active ABZ metabolite sold as ricobendazole, RCB) was included in this study. The use of high-sensitive UHPLC/MS/MS with a triple quadrupole mass analyzer allowed us to identify new metabolites of anthelmintics formed in *H. contortus* adults that have never been described previously.

2. Materials and methods

2.1. Chemicals and reagents

ABZ and RCB was purchased from Sigma-Aldrich (St. Louis, MO, USA). FLU was obtained from Janssen Pharmaceutica (New Brunswick, NJ, USA). Liquid sterile-filtered medium RPMI-1640 medium, HAM F12 medium, Williams' E medium, foetal calf serum and other chemicals (UHPLC, MS or analytical grade) were obtained from Sigma-Aldrich (St. Louis, MO, USA).

2.2. Collection of biological material

One susceptible ISE strain and one resistant IRE strain of *H. contorus* (obtained from Moredun Research Institute) were used in this study. The lambs were bred and used according to protocols which were evaluated and approved by the Ethics Committee of the Ministry of Education, Youth and Sports (Protocol MSMT-25908/2014–9). Six parasite-free lambs (3–4 months old) were orally infected with 5000 third stage larvae (L3) of *H. contortus*. Seven weeks after infection the animals were stunned and immediately exsanguinated in agreement with Czech slaughtering rules for farm animals. Adult nematodes were removed post mortem from the sheep abomasa using the agar method.

2.3. Experimental design

Freshly isolated living *H. contortus* adults were washed three times with phosphate-buffered saline (pH 7.4). Females and males were separated manually under a microscope. Males and females separately

(ten nematodes per one sample) were placed in glass flasks with 5 mL of RPMI medium (pH 7.4, containing $60 \, \mu g \, mL^{-1}$ penicillin and $100 \, \mu g \, mL^{-1}$ streptomycin) and cultivated at 37 °C under humid atmosphere with 5% CO_2. At the beginning of the incubation, 2.5 mL of medium from each flask with the nematodes was removed and the same volume of fresh medium containing 10 μM FLU, ABZ or RCB (pre-dissolved in dimethyl sulfoxide (DMSO)) was added. The final concentration of DMSO in medium was 0.1% (v/v). After a 24-h incubation, the medium was placed into plastic tubes. The nematodes were washed three times with phosphate-buffer saline and were also transferred into the plastic tubes. The samples were frozen and stored at −80 °C. Chemical blanks (medium with anthelmintics, without nematodes) and biological blank samples (medium with nematodes, without anthelmintics) were prepared in the same way.

2.4. Sample preparation

The nematodes were homogenized repeatedly six-times for 10 s in cooled 0.1 M phosphate buffer (pH 7.4) using the FastPrep homogeniser, after which the homogenates were centrifuged at $3000 \times g$ for 5 min. Supernatants of the homogenates as well as medium samples were extracted using the solid-phase extraction (SPE) as described previously (Stuchlikova et al., 2013). Dry samples were quantitatively reconstituted in a mixture of acetonitrile/water (30:70, v/v) using sonication and a vortex for 5 min. One microliter of reconstituted samples was injected into the UHPLC/MS system.

2.5. Proteins concentration measurement

The concentration of protein in the homogenates of the nematodes was measured using bicinchoninic acid assay according to Sigma-Aldrich protocols.

2.6. Analytical conditions of UHPLC-MS/MS

UHPLC (Nexera; Shimadzu, Japan) was optimized using a Zorbax RRHD Eclipse Plus 95 Å C18 column 150 × 2.1 mm, 1.8 μm (Agilent Technologies, Waldrbronn, Germany) at a temperature of 40 °C, flow rate 0.4 mL/min and injection volume 1 μl. The mobile phase consisted of water (A) and acetonitrile (B), both with the addition of 0.1% formic acid (MS grade). The linear gradient was as follows: 0 min–15% B, 8 min–40% B, 10 min–95% B followed by 1 min of isocratic elution. The QqQ mass spectrometer (LC-MS-8030 triple quadrupole mass analyzer; Shimadzu, Japan) was used with the following setting of tuning parameters: capillary voltage 4.5 kV, heat block temperature 400 °C, DL line temperature 250 °C, the flow rate and pressure of nitrogen were 12 l/min, respectively. ESI mass spectra were recorded in the range of m/z 50–1000 in the positive-ion mode, a greater sensitivity for the studied metabolites. The detected metabolites were identified based on the presence of the protonated molecules $[M+H]^+$ and the interpretation of their product ion spectra as described in Supplementary materials. The isolation width $\Delta m/z$ 2 and the collision energy 25 eV (found as optimal energy for fragmentation of studied metabolite ions) were used. Argon was the collision gas for MS/MS experiments. The standards of the potential metabolites were generally not commercially available, and they were not prepared due to the difficulties involved in their synthesis. For this reason, the amounts of metabolites were semi-quantified using a ratio of peak areas for the metabolites, with the area of the internal standard peak (mebendazole (MBZ)). In the homogenates of the nematodes, these ratios were normalized to milligram of total protein. All data are presented as arithmetic mean ± SD (n = 3).

2.7. Statistical analysis

The reported data are expressed as the mean ± S.D. (3–6 replicates). Statistical comparisons were carried out using the Student's t-

Table 1

List of main peaks for FLU biotransformation samples detected by UHPLC-MS/MS with their retention times, theoretical values of $[M+H]^+$ ions in ESI positive-ion mode, elemental composition, product ions, and description of present metabolites.

t_R [min]	Theoretical m/z values of $[M+H]^+$ ions	Elemental composition	Description of metabolite formation		Product ions of $[M+H]^+$, m/z	Metabolite designation
			Phase I	Phase II		
3.22	418.14	$C_{20}H_{20}FN_3O_6$	Hydrolysis	*N*-glycosidation	256, 123	M1$_{FLU}$
3.31	478.16	$C_{22}H_{24}FN_3O_8$	Carbonyl reduction	*N*-glycosidation	316, 284	M2$_{FLU}$
3.42	478.16	$C_{22}H_{24}FN_3O_8$	Carbonyl reduction	*O*-glycosidation	298, 266	M3$_{FLU}$
3.58	478.16	$C_{22}H_{24}FN_3O_8$	Carbonyl reduction	*O*-glycosidation	298, 266	M4$_{FLU}$
3.7	418.14	$C_{20}H_{20}FN_3O_6$	Hydrolysis	*N*-glycosidation	256	M5$_{FLU}$
3.82	478.16	$C_{22}H_{24}FN_3O_8$	Carbonyl reduction	*O*-glycosidation	298, 266	M6$_{FLU}$
4.04	478.16	$C_{22}H_{24}FN_3O_8$	Carbonyl reduction	*N*-glycosidation	316, 284	M7$_{FLU}$
4.8	316.10	$C_{16}H_{14}FN_3O_3$	Carbonyl reduction	–	284, 238	M8$_{FLU}$
5.33	476.14	$C_{22}H_{22}FN_3O_8$	–	*N*-glycosidation	314, 282, 123	M9$_{FLU}$
5.44	330.12	$C_{17}H_{16}FN_3O_3$	Carbonyl reduction	Methylation	298, 174	M10$_{FLU}$
5.52	476.14	$C_{22}H_{22}FN_3O_8$	Hydrolysis, hydroxylation	Glycosidation, O-acetylation	256	M11$_{FLU}$
5.62	476.14	$C_{22}H_{22}FN_3O_8$	–	*N*-glycosidation	314, 282, 123	M12$_{FLU}$
8.27	314.09	$C_{16}H_{12}FN_3O_3$		–	282, 123	FLU (parent drug)

test (GraphPad Prism 7.0). The differences were considered significant at P $<$ 0.05.

3. Results

3.1. Flubendazole

The protonated parent drug FLU is characterized by m/z 314 $[M+H]^+$, retention time 8.27 min and a product ion m/z 282 as the typical neutral loss (NL) of methanol ($\Delta m/z$ 32). Twelve different metabolites of FLU were identified, six of which have heretofore not been described (Table 1, Table 2 and Fig. 1).

FLU with reduced carbonyl group (FLU-R; M8$_{FLU}$) represented the main FLU product of phase I biotransformation. An MS/MS spectrum of the protonated molecule of FLU-R at m/z 316 $[M+H]^+$ resulted in the abundant product ion at m/z 284 (NL of methanol). This metabolite was present in all samples, with significant variations in quantity (see Fig. 2a). Its formation was significantly higher in females than in males, and higher in the IRE than in the ISE strain. In addition to carbonyl reduction, hydroxylation and carbamate hydrolysis of FLU were observed as phase I reactions.

Concerning phase II reactions of FLU, *N*-glycosidation, *O*-glycosidation, methylation and O-acetylation were observed. Two different FLU *N*-glycosides (M9$_{FLU}$, M12$_{FLU}$), two FLU-R *N*-glycosides (M2$_{FLU}$, M7$_{FLU}$), two hydrolyzed FLU *N*-glycosides (M1$_{FLU}$, M5$_{FLU}$) and three FLU-R *O*-glycosides (M3$_{FLU}$, M4$_{FLU}$ and M6$_{FLU}$) were identified. The

characteristic NL for hexose $\Delta m/z$ 162 was observed in tandem mass spectra of all *N*-glycoside conjugates. *O*-glycosides recognition was based on the typical NL of hexose $\Delta m/z$ 162 plus $\Delta m/z$ 18 H_2O. Metabolite M10$_{FLU}$ represents the II phase metabolite which was formed via methylation of FLU-R (M8$_{FLU}$) with the typical NL of methanol. The finding of M11$_{FLU}$ (acetylglycoside of hydrolyzed and hydroxylated FLU) with NL $\Delta m/z$ 220 (*O*-acetyl-glycoside) showed the ability of *H. contortus* to acetylate xenobiotics. The main metabolite of phase II of FLU biotransformation was M4$_{FLU}$ (*O*-glycoside of FLU), which was detected in all samples. Significantly higher amounts of M4$_{FLU}$ were detected in the females than in males. Females of the IRE strain formed a significantly higher amount of this metabolite than females of the ISE strain (see Fig. 2b).

3.2. Albendazole

An MS/MS spectrum of protonated molecule of the parent drug (ABZ, retention time 7.5 min) at m/z 266 $[M+H]^+$ resulted in the abundant product ion m/z 234. Nine ABZ metabolites were detected, four of which have heretofore not been reported (Table 3, Table 4 and Fig. 3).

In phase I, the parent drug was metabolized mainly via a S-oxidation (ABZ.SO; M3$_{ABZ}$) at m/z 282 $[M+H]^+$. As can be seen in Fig. 4a, a significantly lower amount of ABZ.SO was found in the ISE strain than in the IRE strain and in males than in females (with the exception of medium of males). This metabolite was consequently converted via

Table 2

Presence (+) or absence (−) of FLU metabolites in homogenates and medium of *H. contortus* females and males from ISE and IRE strains.

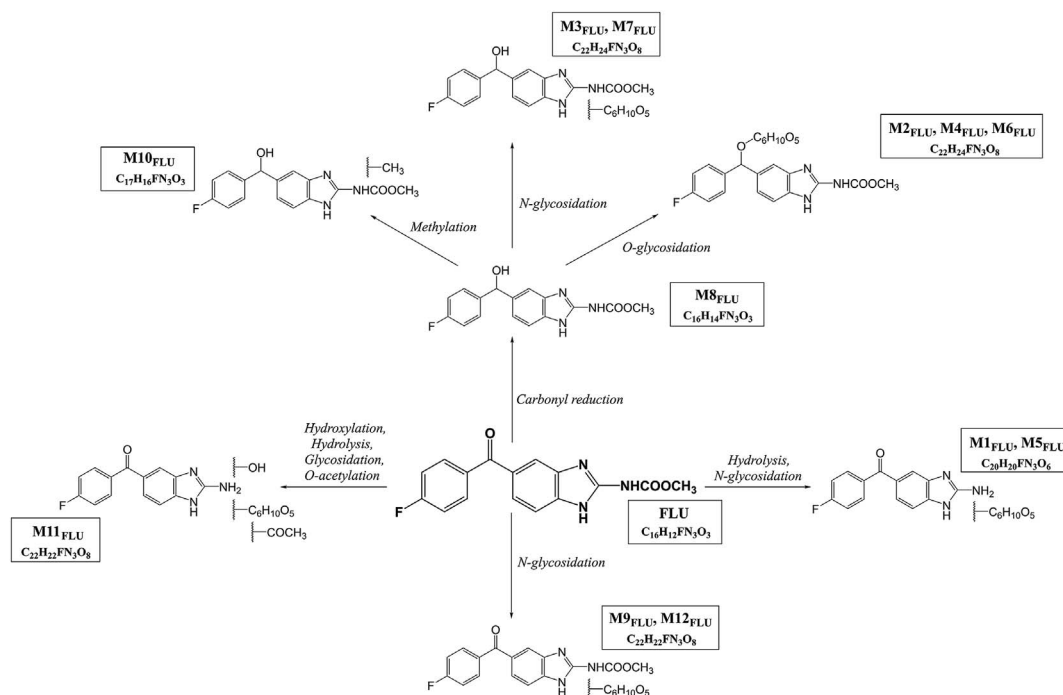| Metabolite designation	Homogenate of *H. contortus*				Medium			
	ISE		IRE		ISE		IRE	
	Females	Males	Females	Males	Females	Males	Females	Males
M1$_{FLU}$	–	–	–	–	–	–	+	–
M2$_{FLU}$	–	–	–	–	–	–	+	–
M3$_{FLU}$	–	–	+	–	–	–	+	+
M4$_{FLU}$	+	+	+	+	+	+	+	+
M5$_{FLU}$	–	–	+	+	+	+	+	+
M6$_{FLU}$	–	–	–	–	–	–	+	–
M7$_{FLU}$	–	–	+	–	+	–	+	–
M8$_{FLU}$	+	+	+	+	+	+	+	+
M9$_{FLU}$	–	–	+	–	–	–	+	–
M10$_{FLU}$	–	–	+	–	–	–	+	+
M11$_{FLU}$	+	+	+	+	+	+	+	+
M12$_{FLU}$	+	+	+	+	+	+	+	+
FLU (parent drug)	+	+	+	+	+	+	+	+

Fig. 1. The proposed metabolic pathway of FLU in *H. contortus* adults.

second S-oxidation to ABZ-sulphone (M6$_{ABZ}$) at m/z 298 [M + H]$^+$. MS/MS spectra contained the typical NL of methanol and $\Delta m/z$ 42 (propene). In addition to S-oxidation, ABZ also underwent a hydrolysis of the carbamate side chain during Phase I biotransformation in *H. contortus*.

Concerning phase II, *N*-glycosidation was the only ABZ biotransformation reported. Three different ABZ *N*-glycosides (M7$_{ABZ}$-M9$_{ABZ}$), two ABZ.SO *N*-glycosides (M1$_{ABZ}$, M2$_{ABZ}$) and two *N*-glycosides of hydrolyzed ABZ (M4$_{ABZ}$, M5$_{ABZ}$) were identified in *H. contortus* adults. The NL of hexose was observed in tandem mass spectra for all these metabolites. The main phase II metabolite, M8$_{ABZ}$ (ABZ *N*-glycoside) was detected in all samples. The amount of this metabolite was significantly higher in the IRE strain than the ISE strain but only in the females. Interestingly regarding ISE strain, the amount of M8$_{ABZ}$ was significantly higher in the males than females (see Fig. 4b).

3.3. Ricobendazole (Albendazole S-oxide)

RCB (albendazole S-oxide, m/z 282 [M + H]$^+$, retention time, 3.32 min) is the anthelmintically active metabolite of ABZ. Seven metabolites of RCB were revealed (Table 5, Table 6 and Fig. 5). In *H. contortus,* RCB underwent two phase I reactions: the reduction of S-oxide and S-oxidation leading to ABZ and ABZ-sulphone formation

(M4$_{RCB}$ and M7$_{RCB}$). In phase II, two *N*-glycosides of RCB (M1$_{RCB}$, M2$_{RCB}$), one *N*-glycoside of ABZ-sulphone (M3$_{RCB}$) and two RCB *N*-glycosides (M5$_{RCB}$, M6$_{RCB}$) were detected with NL of hexose. The comparison of the amounts of the main metabolites (M5$_{RCB}$ and M7$_{RCB}$) are shown in Fig. 6. Significantly higher amounts of both metabolites were found in the IRE strain than the ISE strain and in the females than the males.

3.4. Relative amounts of unmetabolized parent drugs

With the aim to estimate how much of the parent drug was actually metabolized in *H. contortus* adults, the percentage proportion of unmetabolized parent drug was calculated using peak areas (normalized to peak area of IS and to mg of total protein). The sum of normalized peak areas of parent drug and all metabolites in each sample represented 100%. The results are shown in Table 7. In the case of FLU and ABZ, significantly lower amounts of unmetabolized drug were found in females of the IRE strain than in females of the ISE strain. Other differences were not significant due to high inter-individual variability.
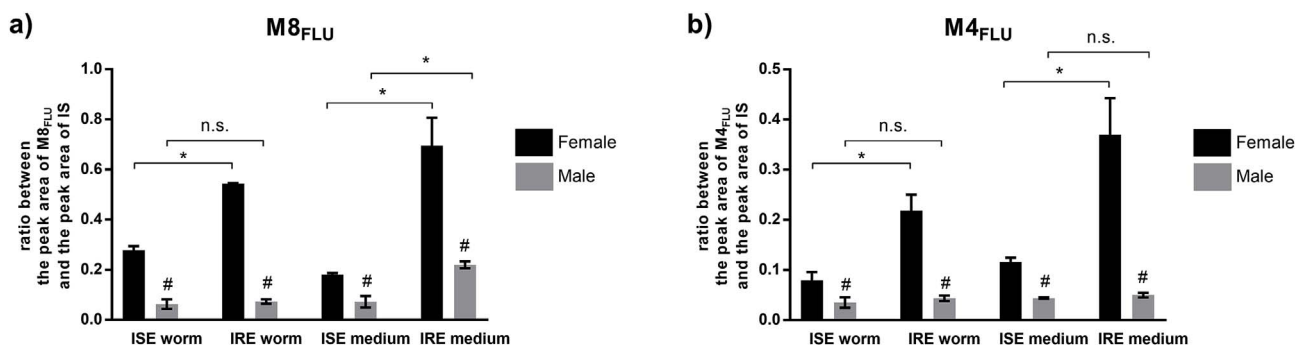

Fig. 2. Changes in the relative amount of the main FLU metabolites M8$_{FLU}$ (FLU-R; Fig. 6a) and M4$_{FLU}$ (FLU-R *O*-glycoside, Fig. 6b) in worm homogenates and medium from females and males of the susceptible ISE strain and resistant IRE strain. The data represent the mean ± S.D. (n = 3). IS = internal standard.

Table 3
List of main peaks for ABZ biotransformation samples detected by UHPLC-MS/MS with their retention times, theoretical values of [M+H]$^+$ ions in ESI positive-ion mode, elemental composition, product ions, and description of present metabolites.

t_R [min]	Theoretical m/z values of [M+H]$^+$ ions	Elemental composition	Description of metabolite formation		Product ions of [M+H]+, m/z	Metabolite designation
			Phase I	Phase II		
1.83	444.14	$C_{18}H_{25}N_3O_8S$	S-oxidation	N-glycosidation	282, 240, 208, 191, 159	M1$_{ABZ}$
2.33	444.14	$C_{18}H_{25}N_3O_8S$	S-oxidation	N-glycosidation	282, 240, 208	M2$_{ABZ}$
3.32	282.09	$C_{12}H_{15}N_3O_3S$	S-oxidation	–	240, 208, 191,159	M3$_{ABZ}$
3.56	370.14	$C_{16}H_{23}N_3O_5S$	Hydrolysis	N-glycosidation	208	M4$_{ABZ}$
4.53	370.14	$C_{16}H_{23}N_3O_5S$	Hydrolysis	N-glycosidation	208	M5$_{ABZ}$
5.22	298.09	$C_{12}H_{15}N_3O_4S$	2*S-oxidation	–	266, 224, 159	M6$_{ABZ}$
5.65	428.15	$C_{18}H_{25}N_3O_7S$	–	N-glycosidation	266, 234, 191	M7$_{ABZ}$
6.16	428.15	$C_{18}H_{25}N_3O_7S$	–	N-glycosidation	266, 234	M8$_{ABZ}$
6.71	428.15	$C_{18}H_{25}N_3O_7S$	–	N-glycosidation	266, 234	M9$_{ABZ}$
7.5	266.10	$C_{12}H_{15}N_3O_2S$	–	–	234	ABZ (parent drug)

4. Discussion

The resistance of *H. contortus* to benzimidazole anthelmintics represents world-wide problem and the mechanisms of benzimidazole resistance in nematodes has been studied for many years. In many molecular studies, changes in target molecule, β-tubulin, have been demonstrated as the primary mechanism of benzimidazole resistance (e.g. Lubega and Prichard, 1990; Lubega and Prichard, 1991; Chaudhry et al., 2015). Occurrence of single nucleotide polymorphisms within three codons (167, 198, and 200) of the β-tubulin isotype-1 gene change the three-dimensional structure of the β-tubulin protein leading to decreased drug binding or decreased affinity of benzimidazoles to target sites. In addition, other mechanisms may contribute to benzimidazole resistance in nematodes, for example, (Vokral et al., 2012, 2013) reported higher levels of metabolism of benzimidazole drugs in resistant compared to susceptible nematodes.

It is well known that the metabolism of anthelmintics in the host affects anthelmintics concentration within parasites (Lifschitz et al., 2017). However, the concentration of biological active anthelmintics in the parasite is also affected by anthelmintics metabolism within parasites themselves (Matouskova et al., 2016). In our previous studies, we identified ABZ and FLU metabolites formed in nematodes *H. contortus* and flukes *Dicrocoelium dendriticum*. Several new worm-specific metabolites, which were not found in hosts, were described. Moreover, significant differences in anthelmintics metabolism between nematodes and flukes were observed (Cvilink et al., 2008; Cvilink et al., 2009).

In the case of *H. contortus*, four metabolites of FLU have previously been described: FLU with reduced carbonyl group (FLU-R), O-glucoside of FLU-R and two N-glucosides of FLU. In the present study, eight new metabolites were identified: N-glycosides of FLU with hydrolyzed carbamate side chain, two N-glycosides of FLU-R, methylated FLU-R, acetylglycoside of hydroxylated FLU with a hydrolyzed carbamate side

chain and two O-glycosides of FLU-R. Most of these new metabolites were surprising, as these metabolic reactions of anthelmintics have not as of yet been described in nematodes. The carbamate hydrolysis of ABZ and FLU has been described in pigs (Bartikova et al., 2010), while the methylation of anthelmintics has been reported only in flukes (Cvilink et al., 2009). The formation of acetylglucosides of the anthelmintics has been identified only in plants (Podlipna et al., 2013; Stuchlikova et al., 2016). In present study, the finding of three different FLU-R metabolites with a molecular mass and fragmentation ions spectrum identical with a metabolite previously identified as O-glucoside of FLU-R was surprising, as FLU-R molecule has only one O-position for sugar binding. Based on identical fragmentation ions, the only difference among these three metabolites can be described in the spatial arrangement of sugar moiety. The finding of three FLU-R-O-glycosides suggests that three different hexoses are conjugated with FLU-R. The use of various sugars in conjugation reactions of xenobiotics and secondary metabolites is known in the plant kingdom, but it has not been described in helminths yet. In any event, this finding brought on several questions, as the previously described glucosides are really glucosides or other glycosides, but structure verification using NMR was not possible due to the low concentration of these metabolites.

Concerning ABZ, four metabolites (ABZ-sulphoxide (ABZ.SO) and three ABZ-N-glucosides) were detected in *H. contortus* adults in our previous study (Cvilink et al., 2008). The formation of ABZ-N-glucosides from ABZ has also been described in the model free-living nematode *Caenorhabditis elegans* (Laing et al., 2010). Owing to the higher sensitivity of the analytical instrument, the present study further revealed five new ABZ metabolites formed in *H. contortus* adults: ABZ-sulphone, two N-glycosides of ABZ with a hydrolyzed carbamate side chain and two ABZ.SO-N-glycosides. As with FLU, it is not certain that the sugar binding to ABZ is glucose or another hexose. For that reason, in present study we decided to name all the conjugates with hexose as

Table 4
Presence (+) or absence (−) of ABZ metabolites in homogenates and medium of *H. contortus* females and males from ISE and IRE strains.

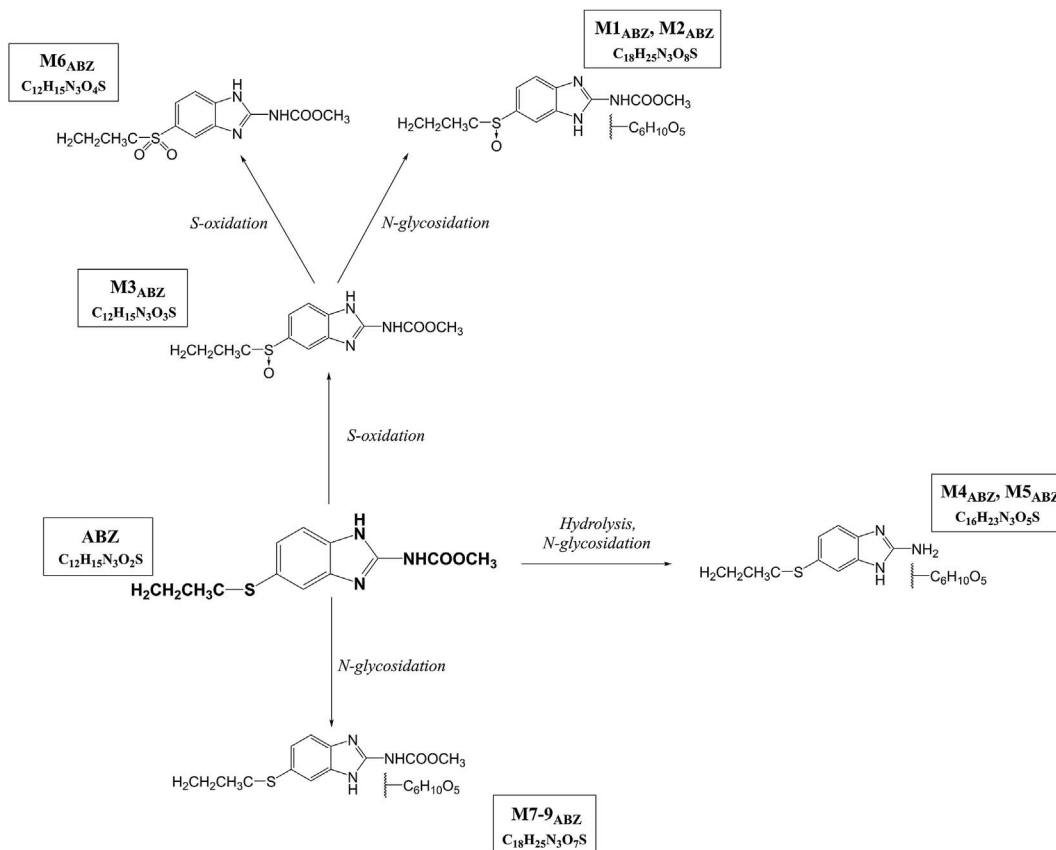| Metabolite designation	Homogenate of *H. contortus*				Medium			
	ISE		IRE		ISE		IRE	
	Females	Males	Females	Males	Females	Males	Females	Males
M1$_{ABZ}$	–	–	+	+	–	–	–	–
M2$_{ABZ}$	–	–	+	+	–	+	+	+
M3$_{ABZ}$	+	+	+	+	+	+	+	+
M4$_{ABZ}$	–	–	–	–	+	+	+	+
M5$_{ABZ}$	–	–	+	–	–	–	+	–
M6$_{ABZ}$	+	+	+	+	+	+	+	+
M7$_{ABZ}$	+	+	+	+	+	+	+	+
M8$_{ABZ}$	+	+	+	+	+	+	+	+
M9$_{ABZ}$	+	+	+	+	–	–	–	–
ABZ (parent drug)	+	+	+	+	+	+	+	+

Fig. 3. The proposed metabolic pathway of ABZ in *H. contortus* adults.

glycosides (rather than glucosides).

RCB metabolism in *H. contortus* has not been studied yet. Seven RCB metabolites were identified in the present study. *H. contortus* adults were able to metabolize RCB via second S-oxidation, S-oxide reduction and *N*-glycosidation. The *N*-glycosides were formed from RCB, ABZ and also from ABZ-sulphone.

The aims of our study were not only to identify new anthelmintic metabolites in *H. contortus* but also to evaluate possible sex-differences. Sex-differences in expression of drug-metabolizing enzymes and drug metabolism are well known in humans as well as farm animals (Waxman and Holloway, 2009; Howard et al., 2015). Sex-differences in the expression of the drug efflux transporter P-gp was reported in parasitic sea lice (Igboeli et al., 2014), but no information has been published regarding sex-differences in drug metabolism in *H. contortus*. Therefore, we compared the metabolic profiles of ABZ, FLU and RCB in females and males of *H. contortus*. The amounts of metabolites were normalized to mg of total protein in order to exclude size-differences in

both sexes. The results showed great sex-differences in the metabolism of all anthelmintics tested. Three detected metabolites (*N*-glycosides) were female-specific ($M7_{FLU}$, $M9_{FLU}$, $M5_{ABZ}$), the formation of several other metabolites differed significantly between males and females. Mostly, a higher amounts of metabolites were found in the females than in males, but one *N*-glycoside of ABZ ($M8_{ABZ}$) was detected in a higher amount in the males than in females. In any event, our results clearly show that there are significant sex-differences in the drug metabolism in *H. contortus* and this fact should be taken into account in all xeno-biotic-metabolism studies in nematodes.

The last aim of our study was to verify the differences in metabolism of benzimidazole anthelmintics between the drug-susceptible and drug-resistant strains of *H. contortus* that we have reported previously (Vokral et al., 2012, 2013). In present study, we tested anthelmintics metabolism separately in females and males of *H. contortus* adults from the ISE and IRE strains. The ISE (MHco3) strain is fully susceptible to anthelmintics and has been adopted as the standard genome strain for
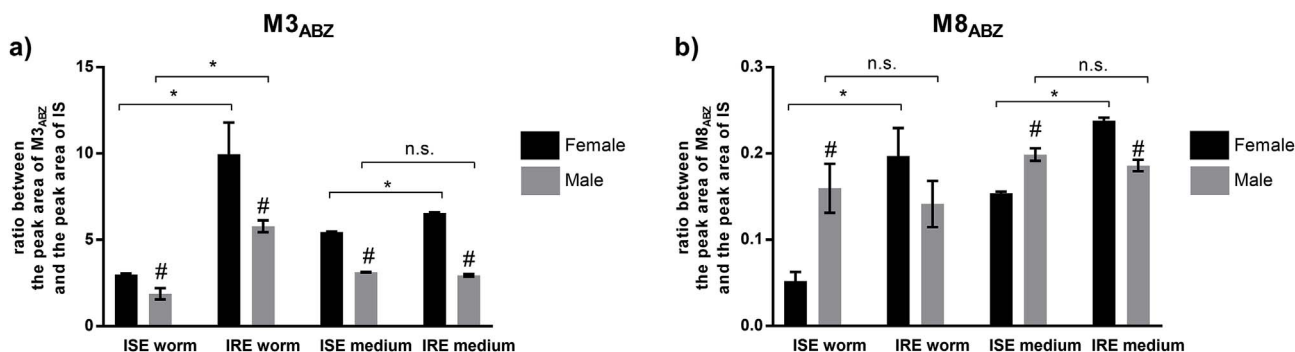

Fig. 4. Changes in the relative amount of the main ABZ metabolites $M3_{ABZ}$ (ABZ.SO; Fig. 2a) and $M8_{ABZ}$ (ABZ-*N*-glycoside, Fig. 2b) in worm homogenates and medium from females and males of the susceptible ISE strain and resistant IRE strain. The data represent the mean ± S.D. (n = 3). IS = internal standard.

Table 5
List of main peaks for RCB biotransformation samples detected by UHPLC-MS/MS with their retention times, theoretical values of [M + H]$^+$ ions in ESI positive-ion mode, elemental composition, product ions, and description of present metabolites.

t_R [min]	Theoretical m/z values of [M + H]$^+$ ions	Elemental composition	Description of metabolite formation		Product ions of [M + H]+, m/z	Metabolite designation
			Phase I	Phase II		
1.83	444.1435	$C_{18}H_{25}N_3O_8S$	–	*N*-glycosidation	282, 240, 208, 191, 159	M1$_{RCB}$
2.33	444.1435	$C_{18}H_{25}N_3O_8S$	–	*N*-glycosidation	282, 240, 208	M2$_{RCB}$
2.88	460.1384	$C_{18}H_{25}N_3O_9S$	S-oxidation	*N*-glycosidation	298, 266, 224	M3$_{RCB}$
5.22	298.0856	$C_{12}H_{15}N_3O_4S$	S-oxidation	–	266, 224, 159	M4$_{RCB}$
5.65	428.1486	$C_{18}H_{25}N_3O_7S$	Reduction of sulfoxide (-O)	*N*-glycosidation	266, 234, 191	M5$_{RCB}$
6.16	428.1486	$C_{18}H_{25}N_3O_7S$	Reduction of sulfoxide (-O)	*N*-glycosidation	266, 234	M6$_{RCB}$
7.5	266.10	$C_{12}H_{15}N_3O_2S$	Reduction of sulfoxide (-O)	–	234	M7$_{RCB}$
3.32	282.09	$C_{12}H_{15}N_3O_3S$	–	–	240, 208, 191, 159	RCB (parent drug)

Table 6
Presence (+) or absence (−) of RCB metabolites in homogenates and medium of *H. contortus* females and males from ISE and IRE strains.

Metabolite designation	Homogenate of *H. contortus*				Medium			
	ISE		IRE		ISE		IRE	
	Females	Males	Females	Males	Females	Males	Females	Males
M1$_{RCB}$	–	–	+	+	–	–	–	–
M2$_{RCB}$	–	–	+	+	–	–	+	–
M3$_{RCB}$	–	–	–	–	–	–	+	–
M4$_{RCB}$	+	+	+	+	+	+	+	+
M5$_{RCB}$	–	–	+	+	–	–	+	+
M6$_{RCB}$	–	–	+	+	–	–	–	–
M7$_{RCB}$	+	+	+	+	+	+	+	+
RCB (parent drug)	+	+	+	+	+	+	+	+

the *H. contortus* sequencing project at the Wellcome Trust Sanger Institute (http://www.sanger.ac.uk/Projects/H_contortus/). The anthelmintic resistant IRE (MHco5) strain (Yilmaz et al., 2017) was directly developed from the ISE strain by the contact of nematodes with anthelmintics. Contrary to previous studies, the multi-resistant strain WR (MHco4) was not included in present study, as the ISE and WR strains have a different origin and are genetically divergent (Redman et al., 2012), thus differences in anthelmintics metabolism between these strains could be related to factors other than drug resistance.

In present *ex vivo* study, the semi-quantification of unmetabolized parent drug and its metabolites showed that 10–72% of anthelmintic drugs present in *H. contortus* adults were metabolized within 24 h. Moreover, the percentage proportion of unmetabolized parent drugs FLU and ABZ was significantly lower in females of IRE than in ISE strain. These facts indicate that the ability to metabolize drug is relatively high in *H. contortus* adults and that the increased drug metabolism could contribute to drug-resistance development in nematodes.

The comparison of the ABZ, RCB and FLU metabolic pathways in the ISE and IRE strains verified that the adults of the resistant IRE strain had a greater ability to deactivate anthelmintics via metabolism than adults of the sensitive ISE strain. Ten identified metabolites were found only in the IRE strain; most of other metabolites were formed in a significantly higher amount in the IRE than in the ISE strain. The nematodes from the IRE strain had more active/expressed enzymes from Phase I biotransformation (oxidases, reductases, hydrolases) as well as from Phase II biotransformation (glycosidation, acetylation). These findings indicate that the enzymes from both biotransformation phases could participate in drug-resistance development in nematodes. The constitutive expression of this CYP34/35 family member (which might catalyze the oxidation of anthelmintics) was reported to be significantly higher in the multiresistant than in susceptible isolates (Yilmaz et al., 2017). Free-living nematodes *Caenorhabditis elegans* metabolized and

excreted the benzimidazole anthelmintics thiabendazole (TBZ), and inhibition of TBZ metabolism increased the susceptibility of *C. elegans* to TBZ (Jones et al., 2015). On the other hand, the accumulation of ABZ.SO and ABZ-sulphone was lower in all ABZ-resistant isolates *Giardia duodenalis* (Arguello-Garcia et al., 2015), a finding which indicates that increased efflux is a more important defense strategy than increased metabolism in some helminth species.

5. Conclusions

The adults of *H. contortus* are able to metabolize the anthelmintics ABZ, RCB and FLU intensively via several biotransformation reactions. Many new anthelmintics metabolites were identified, some of which show new drug biotransformation reactions in nematodes, which have heretofore not been reported. Significant sex-differences in anthelmintics metabolism in *H. contortus* were observed which should be taken into account in xenobiotic metabolism studies in nematodes. Qualitative as well as semi-quantitative comparison of anthelmintics metabolism in the ISE and IRE strains indicate that the metabolism of benzimidazole anthelmintics could be involved in the drug resistance in *H. contortus*.
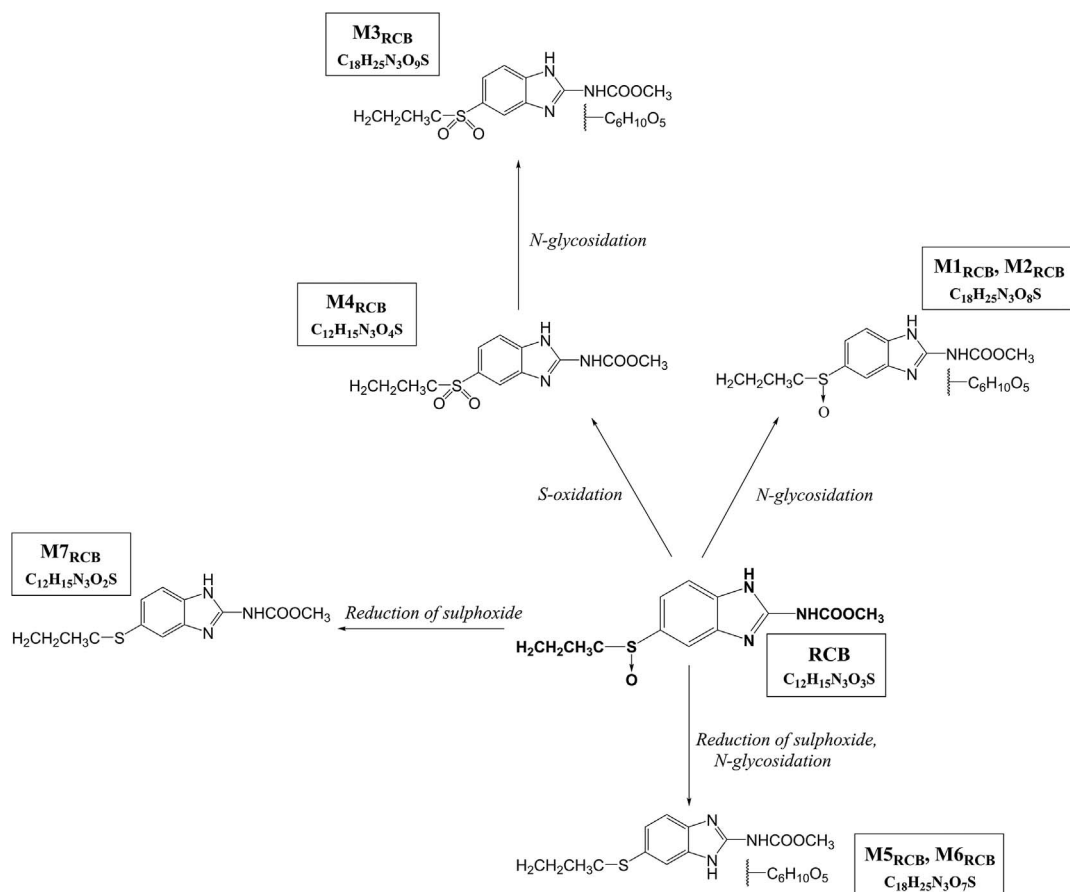
Conflicts of interest

None.

Fig. 5. The proposed metabolic pathway of RCB in *H. contortus* adults.
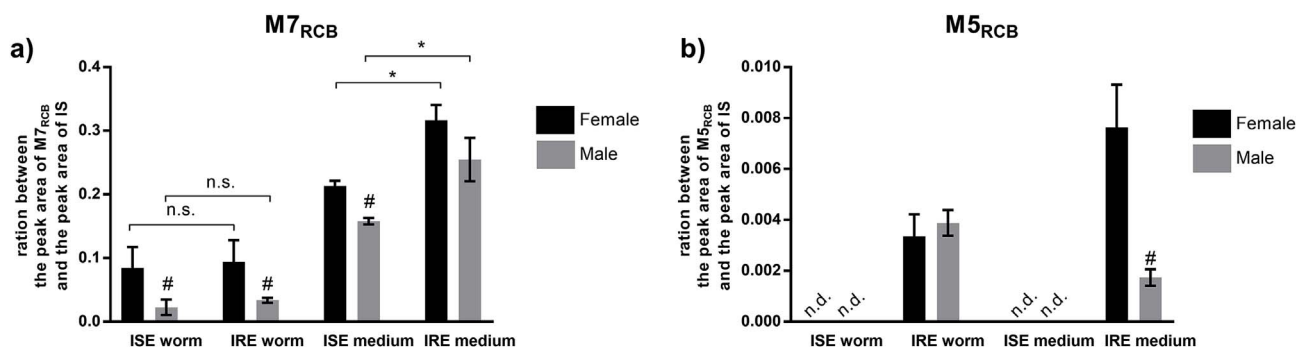

Fig. 6. Changes in the relative amount of the main RCB metabolites M7$_{RCB}$ (ABZ, S-oxide reduction of RCB; Fig. 4a) and M5$_{RCB}$ (glycoside of M7$_{RCB}$, Fig. 4b) in worm homogenates and medium from females and males of susceptible ISE strain and resistant IRE strain. The data represent the mean ± S.D. (n = 3). IS = internal standard.

Table 7
Relative amount of unchanged parent drugs in homogenate of *H. contortus* adults.

	Relative amount of unmetabolized parent drugs [%]			
	ISE		IRE	
	Female	Male	Female	Male
Flubendazole	79.5 ± 6.4	90.3 ± 1.0	58.5 ± 3.8[a]	90.8 ± 8.0
Albendazole	64.2 ± 2.4	81.2 ± 9.3	27.5 ± 3.9[a]	72.6 ± 8.5
Ricobendazole	89.3 ± 11.5	82.1 ± 17.5	87.4 ± 12.6	90.7 ± 6.2

The sum of normalized peak areas of parent drug and all metabolites in each sample represent 100%. The data represent the mean ± S.D. from 3 parallels (n = 3).

[a] Significant difference between females of the ISE and IRE strains, $P < 0.05$.

Appendix A. Supplementary data

Supplementary data related to this article can be found at http://dx.doi.org/10.1016/j.ijpddr.2018.01.005.

References

Arguello-Garcia, R., Cruz-Soto, M., Gonzalez-Trejo, R., Paz-Maldonado, L.M.T., Bazan-Tejeda, M.L., Mendoza-Hernandez, G., Ortega-Pierres, G., 2015. An antioxidant response is involved in resistance of *Giardia duodenalis* to albendazole. Front. Microbiol. 6, 286.

Bartikova, H., Skalova, L., Lamka, J., Szotakova, B., Varady, M., 2010. The effects of flubendazole and its metabolites on the larval development of *Haemonchus contortus* (*Nematoda*: *Trichostrongylidae*): an in vitro study. Helminthologia 47, 269–272.

Brophy, P.M., Mackintosh, N., Morphew, R.M., 2012. Anthelmintic metabolism in parasitic helminths: proteomic insights. Parasitology 139, 1205–1217.

Chaudhry, U., Redman, E.M., Raman, M., Gilleard, J.S., 2015. Genetic evidence for the spread of a benzimidazole resistance mutation across southern India from a single

origin in the parasitic nematode *Haemonchus contortus*. Int. J. Parasitol. 45, 721–728.

Choe, K.P., Leung, C.K., Miyamoto, M.M., 2012. Unique structure and regulation of the nematode detoxification gene regulator, SKN-1: implications to understanding and controlling drug resistance. Drug Metab. Rev. 44, 209–223.

Cvilink, V., Skalova, L., Szotakova, B., Lamka, J., Kostiainen, R., Ketola, R.A., 2008. LC-MS-MS identification of albendazole and flubendazole metabolites formed ex vivo by *Haemonchus contortus*. Anal. Bioanal. Chem. 391, 337–343.

Cvilink, V., Szotakova, B., Vokral, I., Bartikova, H., Lamka, J., Skalova, L., 2009. Liquid chromatography/mass spectrometric identification of benzimidazole anthelminthics metabolites formed ex vivo by *Dicrocoelium dendriticum*. Rapid Commun. Mass Spectr. 23, 2679–2684.

Fernando, L., Furtado, V., Bello, A., Rabelo, E.M.L., 2016. Benzimidazole resistance in helminths: from problem to diagnosis. Acta Trop. 162, 95–102.

Geary, T.G., 2012. Are new anthelmintics needed to eliminate human helminthiases? Curr. Opin. Infect. Dis. 25, 709–717.

Howard, J.T., O'Nan, A.T., Maltecca, C., Baynes, R.E., Ashwell, M.S., 2015. Differential gene expression across breed and sex in commercial pigs administered fenbendazole and flunixin meglumine. PLoS One 10.

Igboeli, O.O., Burka, J.F., Fast, M.D., 2014. Sea lice population and sex differences in P-glycoprotein expression and emamectin benzoate resistance on salmon farms in the Bay of Fundy, New Brunswick, Canada. Pest Manag. Sci. 70, 905–914.

Jones, L.M., Flemming, A.J., Urwin, P.E., 2015. NHR-176 regulates cyp-35d1 to control hydroxylation-dependent metabolism of thiabendazole in *Caenorhabditis elegans*. Biochem. J. 466, 37–44.

Kaminsky, R., Ducray, P., Jung, M., Clover, R., Rufener, L., Bouvier, J., Weber, S.S., Wenger, A., Wieland-Berghausen, S., Goebel, T., Gauvry, N., Pautrat, F., Skripsky, T., Froelich, O., Komoin-Oka, C., Westlund, B., Sluder, A., Maeser, P., 2008. A new class of anthelmintics effective against drug-resistant nematodes. Nature 452 176–U119.

Kotze, A.C., Prichard, R.K., 2016. In: Gasser, R.B., VonSamsonHimmelstjerna, G. (Eds.), Anthelmintic resistance in *Haemonchus contortus*: history, mechanisms and diagnosis. *Haemonchus contortus* and haemonchosis - past, present and future trends. vol. 93. pp. 397–428.

Laing, S.T., Ivens, A., Laing, R., Ravikumar, S., Butler, V., Woods, D.J., Gilleard, J.S., 2010. Characterization of the xenobiotic response of *Caenorhabditis elegans* to the anthelmintic drug albendazole and the identification of novel drug glucoside metabolites. Biochem. J. 432, 505–514.

Lifschitz, A., Lanusse, C., Alvarez, L., 2017. Host pharmacokinetics and drug accumulation of anthelmintics within target helminth parasites of ruminants. New Zealand Vet. J. 65, 176–184.

Lubega, G.W., Prichard, R.K., 1990. Specific interaction of benzimidazole anthelmintics with tubulin-high affinity binding and benzimidazole resistance in *Haemonchus contortus*. Mol. Biochem. Parasitol. 38, 221–232.

Lubega, G.W., Prichard, R.K., 1991. Beta-tubulin and benzimidazole resistance in the sheep nematode *Haemonchus contortus*. Mol. Biochem. Parasitol. 47, 129–137.

Matouskova, P., Vokral, I., Lamka, J., Skalova, L., 2016. The role of xenobiotic-metabolizing enzymes in anthelmintic deactivation and resistance in helminths. Trends Parasitol. 32, 481–491.

Podlipna, R., Skalova, L., Seidlova, H., Szotakova, B., Kubicek, V., Stuchlikova, L., Jirasko, R., Vanek, T., Vokral, I., 2013. Biotransformation of benzimidazole anthelmintics in reed (*Phragmites australis*) as a potential tool for their detoxification in environment. Biores. Technol. 144, 216–224.

Raza, A., Lamb, J., Chambers, M., Hunt, P.W., Kotze, A.C., 2016a. Larval development assays reveal the presence of sub-populations showing high- and low-level resistance in a monepantel (Zolvix (R))-resistant isolate of *Haemonchus contortus*. Vet. Parasitol. 220, 77–82.

Raza, A., Bagnall, N.H., Jabbar, A., Kopp, S.R., Kotze, A.C., 2016b. Increased expression of ATP binding cassette transporter genes following exposure of *Haemonchus contortus* larvae to a high concentration of monepantel in vitro. Parasites Vectors 9, 522.

Redman, E., Sargison, N., Whitelaw, F., Jackson, F., Morrison, A., Bartley, D.J., Gilleard, J.S., 2012. Introgression of ivermectin resistance genes into a susceptible *Haemonchus contortus* strain by multiple backcrossing. PLoS Pathog. 8, e1002534.

Roos, M.H., Otsen, M., Hoekstra, R., Veenstra, J.G., Lenstra, J.A., 2004. Genetic analysis of inbreeding of two strains of the parasitic nematode *Haemonchus contortus*. Int. J. Parasitol. 34, 109–115.

Sales, N., Love, S., 2016. Resistance of Haemonchus sp to monepantel and reduced efficacy of a derquantel/abamectin combination confirmed in sheep in NSW, Australia. Vet. Parasitol. 228, 193–196.

Srivastava, M., Misra-Bhattacharya, S., 2015. Overcoming drug resistance for macro parasites. Future Microbiol. 10, 1783–1789.

Stuchlikova, L., Jirasko, R., Skalova, L., Pavlik, F., Szotakova, B., Holcapek, M., Vanek, T., Podlipna, R., 2016. Metabolic pathways of benzimidazole anthelmintics in harebell (*Campanula rotundifolia*). Chemosphere 157, 10–17.

Stuchlikova, L., Jirasko, R., Vokral, I., Lamka, J., Spulak, M., Holcapek, M., Szotakova, B., Bartikova, H., Pour, M., Skalova, L., 2013. Investigation of the metabolism of monepantel in ovine hepatocytes by UHPLC/MS/MS. Anal. Bioanal. Chem. 405, 1705–1712.

Taman, A., Azab, M., 2014. Present-day anthelmintics and perspectives on future new targets. Parasitol. Res. 113, 2425–2433.

Vokral, I., Bartikova, H., Prchal, L., Stuchlikova, L., Skalova, L., Szotakova, B., Lamka, J., Varady, M., Kubicek, V., 2012. The metabolism of flubendazole and the activities of selected biotransformation enzymes in *Haemonchus contortus* strains susceptible and resistant to anthelmintics. Parasitology 139, 1309–1316.

Vokral, I., Jirasko, R., Stuchlikova, L., Bartikova, H., Szotakova, B., Lamka, J., Varady, M., Skalova, L., 2013. Biotransformation of albendazole and activities of selected detoxification enzymes in *Haemonchus contortus* strains susceptible and resistant to anthelmintics. Vet. Parasitol. 196, 373–381.

Waxman, D.J., Holloway, M.G., 2009. Sex differences in the expression of hepatic drug metabolizing enzymes. Mol. Pharmacol. 76, 215–228.

Yilmaz, E., Ramunke, S., Demeler, J., Krucken, J., 2017. Comparison of constitutive and thiabendazole-induced expression of five cytochrome P450 genes in fourth-stage larvae of *Haemonchus contortus* isolates with different drug susceptibility identifies one gene with high constitutive expression in a multi-resistant isolate. Int. J. Parasitol. Drug. Drug Resist. 7, 362–369.